Design of robust PI controller by combining robustness regions with time-domain criteria

Vilém Žán, Karel Kubíček, Martin Čech
NTIS – New Technologies for the Information Society
Faculty of Applied Sciences, University of West Bohemia
Technická 8, 306 14 Plzen, Czech Republic
E-mail: vzan@students.zcu.cz, lerry482@ntis.zcu.cz, mcech@ntis.zcu.cz

***Abstract*—This paper describes the design of a robust PI controller by considering several design criteria simultaneously (multi-objective optimization). Firstly, all controllers satisfying multiple frequency domain criteria (*e.g.* sensitivity function limits) are found in PI parameter plane using robustness regions method. Then, all suitable controllers are evaluated by the selected time-domain criterion, for example: Integral Error (IE), Integral of Time-weighted Absolute Error (ITAE) etc. Further, application of $\mathbf{H_2}$ and $\mathbf{H_\infty}$ norms is shown in that context. The whole design toolchain is supported by advanced Matlab GUI which was used in the illustrative example. The described approach can be extended for PID controllers as well, for development of advanced autotuners and for teaching and training purposes.**

***Index Terms*—frequency domain, multi-objective optimization, Nyquist plot shaping, PI controller, PID controller, process control, robustness regions, time domain, $\mathbf{H_\infty}$ approach**

I. Introduction

It is well reported that feedback control can bring huge energy and material savings as well as other economic benefits. Consequently, many methods and theories on how to set feedback controller parameters have emerged. Their number varies depending on the type of the used controller. With increasing controller complexity (in terms of parameters and structure), it is highly difficult to tune and implement it properly. Therefore, proportional-integral (PI) and proportional-integral-derivative (PID) controllers are still the most widely used not only in process control but also in energetic, robotics and other fields. Literature states that almost 90% of all cases are PID controllers [1]. Majority of them (97%) do not use derivative term, *i.e.* are just PI type. Surprisingly, still many of these PI controllers (70%) are tuned improperly [2] or work just with default parameters hence do not bring expected savings and product quality (see *e.g.* [3]).

The *Ziegler-Nichols* method is one of the oldest experimental methods [1]. However, during the evolution of industrial technology, these methods were proven to give often unstable feedback loop. Hence it was necessary to find more exact analytical approaches. General overview of PID control system analysis, design, and technology is given *e.g.* in [4]. Some of the classical design methods in time and frequency domain, both analytical or numerical are described in [5]. Some of the approaches are quite specific, *e.q.* fuzzy PID controller [6]. The time-domain optimality of feedback loops can be analyzed by different criteria. One of the most popular is ITAE, see for example [7]. Over the time, also model uncertainties were included in the design process, mainly to reflect unmodelled dynamics of the real system. This led to the development of methods for robust control [8]. For example, robust PI controller is often designed using a normalized process model and the constant stability margins and crossover frequency in the parameter space [2]. Another approaches are based on Hurwitz-Stability and Gamma-Stability [9]. A robust controller can be also designed using H_∞ norm [8, 10, 11]. Robust controller design brings a lot of principal trade-offs which are discussed in [12]. It is always usefull to have some *a priori* information about physical nature of the real system. The robust design based on robustness regions has a wide range of applications: a continuous stirred tank reactor [13], battery-supercapacitor energy storage system [14] or large wind turbine with communication delays [15].

This paper brings a method which combines robustness regions method with time domain optimization. It allows Nyquist curve or sensitivity function shaping for multiple shaping points [8]. Firstly, the design of the controller is carried out in frequency domain. Here all controllers satisfying given shaping conditions are found. They represent a robustness region in controller parameter plane [16, 17, 18]. All controllers from the region are evaluated using selected time-domain criterion, for example: Integral Error (IE), Integral of Time-weighted Absolute Error (ITAE) etc. In this paper, six time-domain criteria will be considered. Additionally, the analysis of the obtained robust region will be performed using H_2 and H_∞ norms. Due to the considerable complexity of the calculations, a GUI toolbox was created. It was implemented in Matlab and it contains all the calculations, making it an easy-to-use for any user. Such GUI allows also to include more complex user-defined functions.

Paper is organized as follows: Section II will introduce the basic concepts of process control and robust controller design. The following Section III will describe how to obtain a robustness region. Subsequently, it will be described here how the intersection of the regions is computed for several considered shaping points simultaneously. The considered various criteria will be described here. Section IV is devoted to a simulation example on which the whole process will be documented. Section V describes potential improvements. Section VI brings conclusions.

II. Problem formulation

A. Process and controller model

Figure 1 shows the classical structure of a closed control loop [1]. The process is considered as linear, and it is described by a transfer function $P(s)$. The $C(s)$ block represents the linear controller.

The signal $r(t)$ represents the reference value. $e(t)$ represents the control error. The output is represented by a $y(t)$ signal. The signals $d_1(t)$ and $d_2(t)$ are the input and output noise/disturbances that affect the system. Typically, this may be due to inaccuracies in the sensors and actuators.

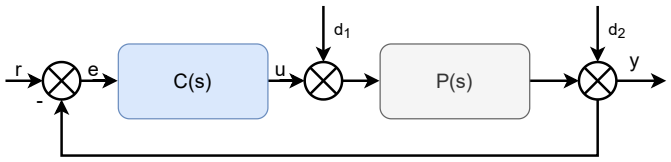

Fig. 1. The classic structure of the closed-loop control system

The controller $C(s)$ may have many variant forms. However, this article is limited only to the PI controller, which has the following transfer function [5]:

$$C(s) = K_p + \frac{K_i}{s},$$

where K_p represents the gain of the proportional term and K_i is the gain of the integral term. The open loop of the system shown in Figure 1 can be written as:

$$L(s) \triangleq C(s)P(s).$$

The closed-loop has the following transfer function $T(s)$. It can be referred to as a *complementary sensitivity function*:

$$T(s) \triangleq \frac{L(s)}{1+L(s)} = \frac{C(s)P(s)}{1+C(s)P(s)}.$$

The *sensitivity function* $S(s)$ then has the form:

$$S(s) \triangleq \frac{1}{1+L(s)} = \frac{1}{1+C(s)P(s)}.$$

B. Design specifications

Before the controller is designed, it is always necessary to specify the goal which has to be achieved. In the vast majority of cases, the most important is the closed-loop stability of a given system [19]. Additionally, it can be, for example, performance of a load disturbances response, set point response and robustness against uncertainties in the considered model [11]. These requirements can be characterized by a formula:

$$||H(s)||_\infty < \gamma. \tag{1}$$

Suppose that $H(s)$ in this case represents a stable closed-loop transfer function of a given system. The γ is a parameter which has a relation to robustness-performance trade-off. $H(s)$ infinity norm can be written in following form where ω indicates frequency.

$$||H(s)||_\infty \triangleq \sup_\omega |H(j\omega)| \tag{2}$$

In this article, the following controller design conditions will be considered [8]:

$$||W_S(s)S(s)||_\infty < \gamma_S, \tag{3}$$
$$||W_T(s)T(s)||_\infty < \gamma_T, \tag{4}$$

where $W_S(s)$ and $W_T(s)$ are considered as stable rational functions with no poles on the imaginary axis. They are often referred to as "weighting functions". In the specific case where $W_S(s) = W_T(s) = 1$, $\gamma_S = M_S$ and $\gamma_T = M_T$. Then the (4) and (3) can be rewritten into a form:

$$||S(s)||_\infty < M_S,$$
$$||T(s)||_\infty < M_T.$$

1) Conditions for H_∞ controller: If the controller $C(s)$ is designed using H_∞ approach then it must meet the following conditions [8]:

- the closed-loop system is stable,
- the transfer function $H(s)$ is stable,
- the inequality constraint (1) must be satisfied for a given design parameter $\gamma > 0$.

Another way how to ensure robustness is to define several shaping points in the Nyquist plot plane. Then the region boundary in K_p - K_i is calculated using the following formulas [11, 20]:

$$K_p(\omega) = \frac{a(\omega)u + b(\omega)v}{a^2(\omega) + b^2(\omega)}, \tag{5}$$
$$K_i(\omega) = \frac{\big[b(\omega)u - a(\omega)v\big]\omega}{a^2(\omega) + b^2(\omega)}, \tag{6}$$

where $a(\omega) = \mathrm{Re}P(j\omega)$, $b(\omega) = \mathrm{Im}P(j\omega)$. $P(j\omega)$ represents system process, u and v represent shaping point in complex plain for $L(j\omega) = u + \mathrm{j}v$. Parameter ω indicates frequency.

2) Additional evaluation criteria in the time domain: The obtained region contains an infinite number of controllers. It is therefore appropriate to supplement this procedure with the additional evaluation criteria [1, 11, 21]. The following six criteria will be considered in this article.

- **IE** – Integral of Error

$$IE = \int_0^{+\infty} e(t)dt,$$

- **ITE** – Integral of Time Error

$$ITE = \int_0^{+\infty} t \cdot e(t)dt,$$

- **ISE** – Integral of Square Error

$$ISE = \int_0^{+\infty} e^2(t)dt,$$

- **IAE** – Integral of Absolute Error

$$IAE = \int_0^{+\infty} |e(t)|dt,$$

- **ITAE** – Integral of Time Absolute Error

$$ITAE = \int_0^{+\infty} t \cdot |e(t)|dt,$$

- **IGSE** - Integral of Generalized Square Error - α represents a subjectively selected weighted parameter. This criterion provides better results than ISE [21].

$$IGSE = \int_0^{+\infty} [e^2(t) + \alpha \cdot \dot{e}^2(t)]dt.$$

The obtained robustness region is sampled, and all controllers are numerically evaluated *via* above described criteria. This process will be described in detail in the following chapters and also in a simulation example IV.

3) System norms for evaluation of the closed loop: Another way to evaluate the resulting region is to implement the calculation of the norms for the system. The closed-loop system will be denoted as $H(s)$. Only the two system norms will be described in more detail. They will be the H_2 norm ($||H||_2$) and the H_∞ norm ($||H||_\infty$).

- **H_2 norm -** The H_2 signal norm represents the energy it contains. The H_2 system norm can thus serve as a design criterion for optimizing the resulting price function.

$$||H||_2 \triangleq \left(\frac{1}{2\pi}\int_{-\infty}^{+\infty} |H(j\omega)|^2 d\omega\right)^{\frac{1}{2}}. \quad (7)$$

- **H_∞ norm -** H_∞ norm represent the maximum singular value of the function over that space. For H_∞ norm of the signals this means maximum gain. This can be interpreted as a maximum gain in any direction and at any frequency. If the system is a stable single input and single output (SISO) system then the H_∞ norm is the peak gain, the largest value of the frequency response magnitude. The H_∞ norm prescription is given in the equation (2).

III. Design criterion for PI controller

The process of obtaining the robust regions will be introduced in this chapter. As it was described earlier, the border of the robust region for PI controller is a parametric curve calculated in $[K_i, K_p]$ plane from equations (5), (6). Inputs of these equations are real $a(\omega)$ and imaginary $b(\omega)$ parts of given process. And then there are the shaping points defined as $u + jv$. Where u is real part and v is imaginary part of shaping point in the complex plane.

One of the primary advantages of this method is that several design criteria can be expressed as a shaping point represented by the u, v coordinates. Few of these main frequency domain design criteria can be seen in following Table I [20]. These criteria are often considered and used in control theory.

TABLE I
Design criteria

Design criteria	Label
Gain margin	G_M
Phase margin	P_M
Sensitivity function (SF) limit	M_S
Complementary sensitivity function (CSF) limit	M_T
Low-frequency disturbance rejection	ε_S
Bandwidth of the control loop	ε_T

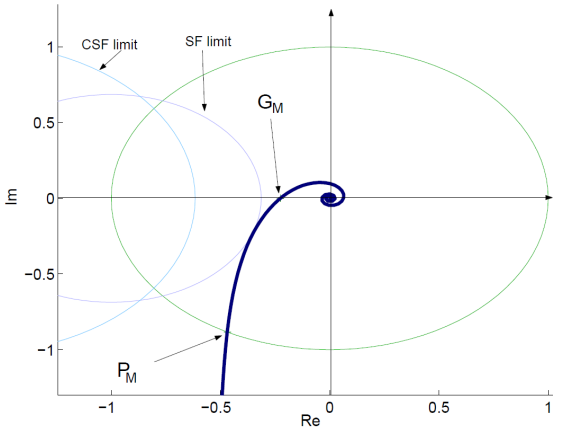

Fig. 2. Nyquist plot shaping based on design criteria [11]

Design criteria noted in Table I pictured as a shaping points can be observed in the Figure 2 (the geometric interpretation). The green circle represents the unit circle.

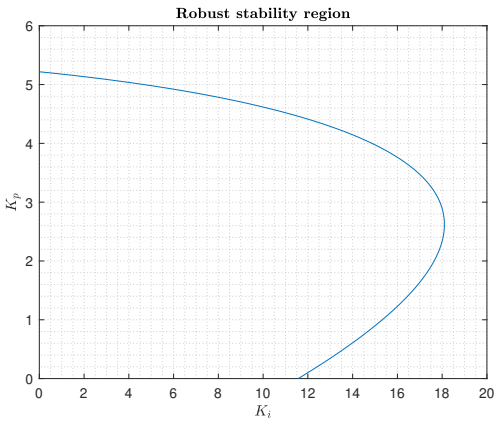

Fig. 3. Illustration of robust stability region representing GM criterion

Particular robustness region is obtained for each shaping point (*i.e.* design criteria). The region contains parameters of stabilising controllers which satisfy defined criteria. One of the robust stability regions is shown in Figure 3.

However, multiple criteria can be selected, and thus multiple regions can be obtained. This fact is illustrated in Figure 4. In this case, three shaping points were chosen as will be shown in Table II in Simulation examples IV. These points will be considered throughout the rest of the paper. Intersection of these regions represents parameters of stabilising controllers satisfying all required design criteria.

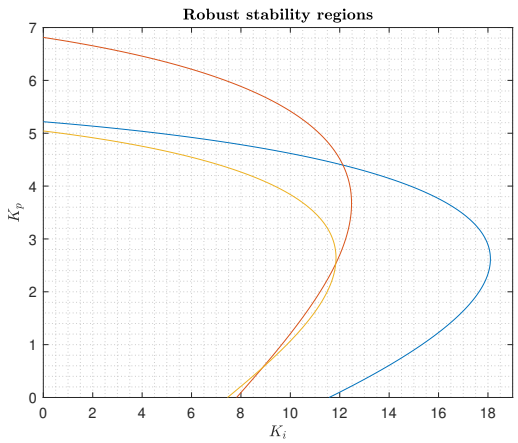

Fig. 4. Illustration of robust stability region representing three design criteria

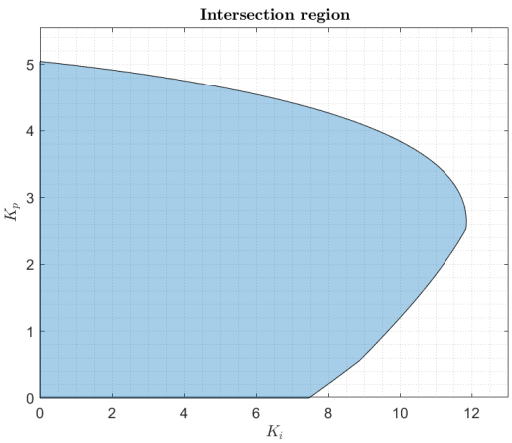

Fig. 6. The resulting intersection of three regions

A. *Intersection of several regions*

Each shaping point provides its own robust regions. Subsequently, their intersection and its evaluation will be performed. Figure 5 shows the regions for the three shaping points considered. Their mutual intersections are color-coded. The red-brown area (in the lower left quarter) of the graph indicates the controllers that meet the requirements for all three shaping points.

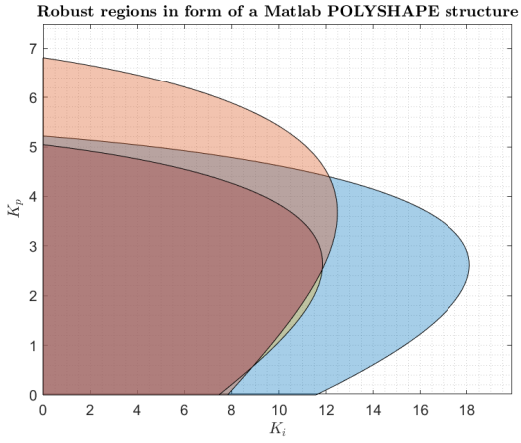

Fig. 5. Polyshape regions for multiple shaping points

Thus, only the part for which all design requirements are met is considered for further processing of the simulation. The final form of the final region, which was created by the intersection of three, is presented in Figure 6. For further processing of the region, it is necessary to sample it - that is, to sample the parameters K_i and K_p. Sampling fineness represents an optional parameter. The finer it is selected, the more controllers will be contained in the resulting region, but the computational complexity of the whole operation will increase significantly.

Furthermore, the resulting region will be firstly evaluated using six time domain criteria. Additionally, the region will be evaluated using the system norms for each PI controller that occurs in the region. The region was sampled as a mesh grid matrix with its limits set as the maximal values of K_i, K_p coordinates of the region. However, this sampling did not respect irregular shape of the region creating a rectangular grid. Cubic approximation of the sampled region had to be performed on the obtained rectangular grid. As a result, it is then possible to represent any irregular shape of the region for its further processing. The sampled area is shown in Figure 7. Current sampling has been set to three hundred samples of region coordinates $[K_i, K_p]$. This sampling option will be equally used in the case of the simulation example.

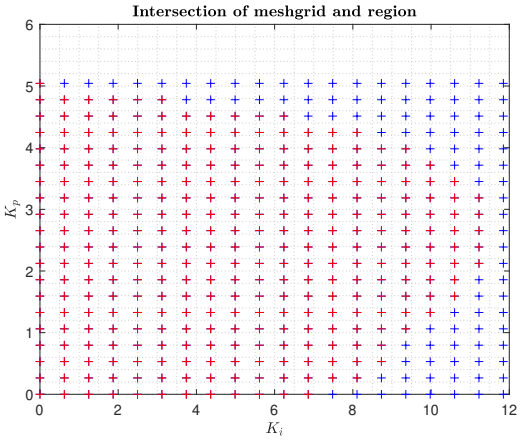

Fig. 7. Sampled area of the intersection region

All mentioned time criteria in II-B2 and II-B3 were numerically computed for each sampled point of the obtained approximated plane resulting in 3-dimensional graph. The simulation was performed using model created in Matlab and Simulink. The aim was to find minimal values of all time criterion which were easily observable in the 3-dimensional graph. For better understanding, these graphs will be shown only in a simulation example.

IV. Simulation example

The following system will be considered to evaluate the proposed approach. It is a system with two poles, one zero and a time delay.

$$P(s) = \frac{(s+1)}{(s+2)(s+3)} e^{-0.2s}$$

The step response of the system is shown in Figure 8. It is evident from the graph that this is a stable system with time delay, but it has a significant overshoot. Overshoot can be easily compensated by the controller.

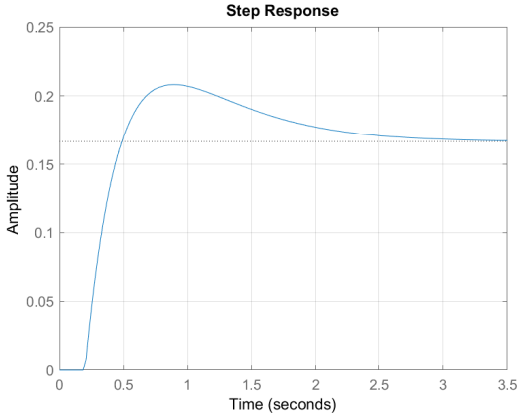

Fig. 8. Step response plot of the example system

Bode plot of the system is shown in Figure 9.

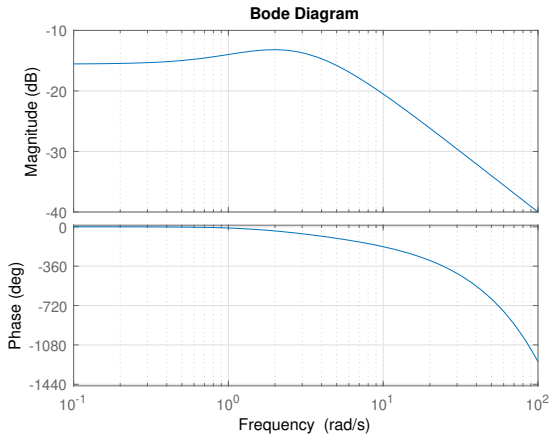

Fig. 9. Bode plot of the example system

The following step is to perform an analysis of the considered system $P(s)$ by calculating its H_2 and H_∞ norms. The calculations were carried out according to the formulas (7) and (2). The frequency at which the system reaches its maximum value (H_∞) is 1.9953.

$$||P(s)||_2 = 0.3416 \qquad ||P(s)||_\infty = 0.2193$$

All calculations and simulations were performed on a computer with CPU I7 - 8700k 3.70GHz, 16GB RAM, 2TB HDD and Windows 10 64bit.

The design requirements for the gain margin will be considered as $G_M = 2$. The phase margin will be set to $P_M = 60$ degrees. The maximum value of the sensitivity function will be required as $M_S = 1.6$. Considered design criteria are listed in Table I. Each of these requirements can be represented by a shaping point. In that manner, a robust region that satisfies it will be obtained for each shaping point. The individual shaping points are listed in Table II. In total, there are three points considered at once but any number of shaping points can be considered here. It depends on the specific requirements of the designer and the considered shape of the system.

TABLE II
Shaping points

Index of point	Coordinates	Design criteria
1. point	$0 - 0.5j$	$G_M = 2$
2. point	$-0.5 - 0.866j$	$P_M = 60°$
3. point	$-0.5 - 0.375j$	$M_S = 1.6$

A robust region is therefore obtained for each point. All three regions are shown in the Figure 4. It contains controllers that meet the requirement. The resulting region is obtained by the intersection of three robust regions. Their intersection is then color-coded in Figure 5. The resulting region for this example is depicted in Figure 6. This resulting region was sampled in the same manner as described in Section III-A. Its shape is displayed in Figure 7. If multiple shaping points were selected, the whole process would not change. This fact would be reflected solely in the part for obtaining the resulting region. It would be created by the mutual intersection of the considered number of shaping points (regions). As a result, the intersection region can have a much more complex shape, which is given by the intersection of all regions. In the case of more complex shapes, it might be necessary to improve the approximation method of the shape of this irregular region.

Subsequently, a simulation was created in Matlab Simulink, where all the obtained controllers were evaluated according to the chosen time criteria. Six criteria were considered, which were described in Chapter II-B2. The resulting graphs are shown in Figure 10. On the top left 10 is the graph for the IE criterion. To the right of it is a graph for the ITE criterion. The second row from the left in 10 shows the graph for ISE. To the right is the graph for IAE. The last row in 10 from the left shows the graph for ITAE. To the right is the graph for IGSE. The α parameter was selected with a value of 0.5. It is evident from the graphs that the calculation of the criterion took place only on the defined sampled resulting region.

The graphs depicted on the Figure 10 show that all chosen criteria provide similar information. The more fundamental difference between them is only in the steepness as the criterion grows. This is primarily due to the contemplated shape of the system that was used as an example. In the case of a more complex system, it would be possible to obtain graphs with a various shapes. The criteria for ITE and ITAE achieve the highest values for example system. Furthermore, for example, the ISE criterion provides the steepest course. Also worth mentioning here is the design parameter α in the

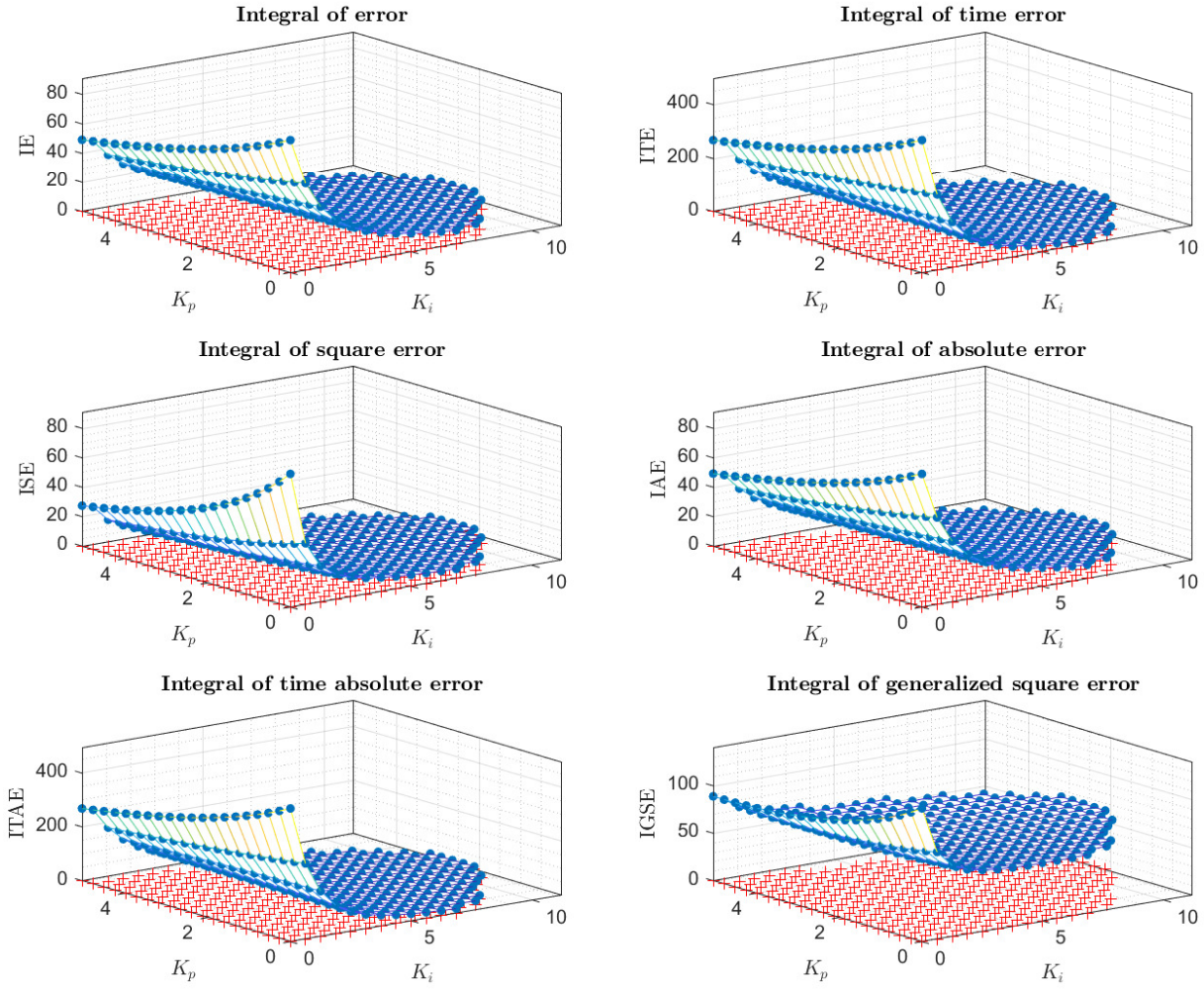

Fig. 10. 3D visualisation of integral criteria for the final robust region. On the top are the IE and ITE criteria. ISE and IAE are in the middle row. At the bottom are ITAE and IGSE.

case of IGSE. If it had been chosen differently, the graph would have looked different. These graphs thus provide an interesting insight into the evaluation of the resulting region. In the same way, it depends on the specific application, where designers may be interested only in some of the criteria listed. Their results can be further used for other operations. For example, it may be another analysis that can be used in another optimization process.

The subsequent step in evaluating the resulting region will be the usage of the H_2 and H_∞ norms for a closed-loop system. The calculations were performed according to the formulas (7) and (2) again. Even in this case, the resulting region was composed of three hundred controllers as in the previous case. The values obtained for both norms are displayed in Figure 11. In the Figure 11 on the left, the resulting region is evaluated using the H_2 norm. On the right, the resulting region is evaluated by the H_∞ norm. The results for the H_2 norm show that as the value for K_i and K_p increases then the total energy of the system also increases. In the case of the results for the H_∞ norm, it is clear that almost all controllers are evaluated at 1. This means the specified controller stabilizes the system and reaches the required value. In this manner, it converges to the value of the set point. Only the values for $K_i = 0$ do not achieve the value of 1. These controllers do not attain the required value when it is caused by the absence of the integration component in the controller. Consequently, only the proportional component is present there, which is not enough to reach the set point. In this case, the considered PI controllers changed only to P. This fact stems mainly from the shape of the resulting region.

From the resulting graphs, it is straightforward that only the graph for H_2 norms provides interesting results. The controllers can be divided according to the total energy. Based on the analysis, a regulator can be selected that meets the specified requirement for total energy, the definition of which depends on the specific application. In contrast, the graph for

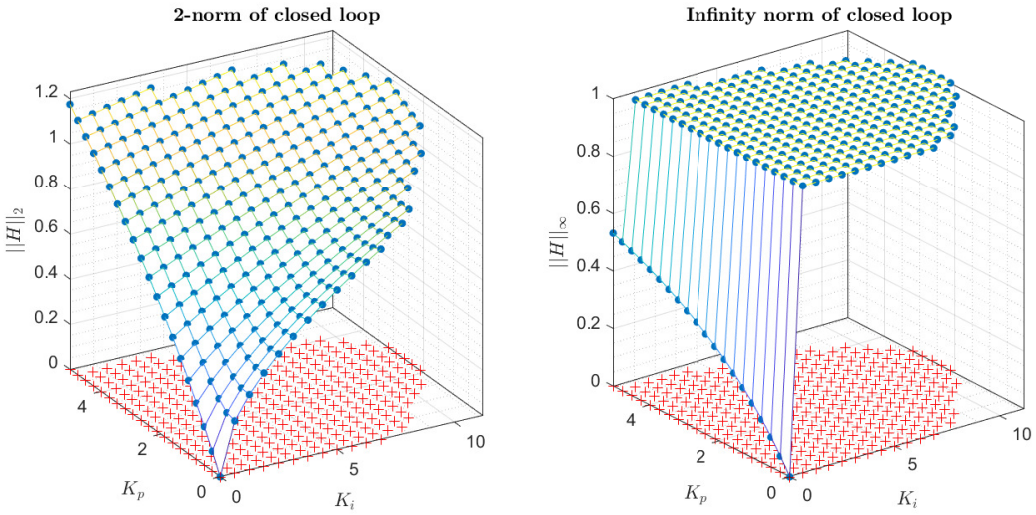

Fig. 11. 3D visualisation of $||H||_2$ and $||H||_\infty$ of the closed-loop obtained from the parameters of the final robust region and defined nominal process. On the left there is 2-norm of the closed-loop. On the right there is ∞-norm of the closed-loop.

H_∞ only provides information on convergence to the desired value, but nothing more. The question arises of whether it makes sense to plot such graphs. On the other hand, it is clearly displayed at first glance whether the regulators contained in the resulting region are actually converging to the required value.

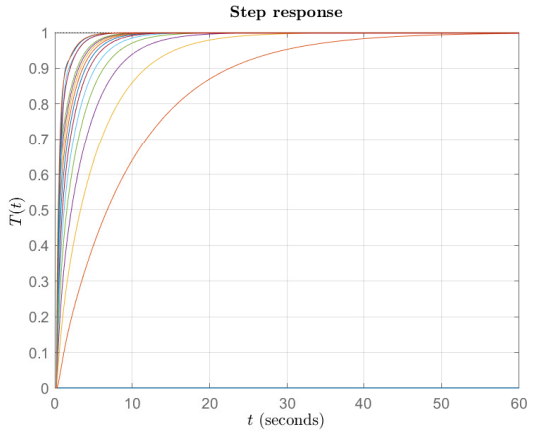

Fig. 12. Step response of selected closed-loop systems computed from the final robust region.

To verify the results, a simulation was performed for thirty closed-loops. They were selected from a total of three hundred in such a way that it started from the first, then continued with a step of ten to three hundred. The simulation was performed in Matlab, and it was a step response simulation for each system. The results are presented in Figure 12.

From the results, it can be found that some controllers take up to 200s before they achieve the required value. This fact is illustrated by the blue line in the Figure 12 which is close to 0 throughout the 60s shown and grows only very slowly. Other selected controllers are faster. This fact is related to the graph on the left of the Figure 11 for the H_2 norm.

V. Future works

First of all, the authors plan to test the GUI on more complex models and also on some real systems. When switching to more complex systems also more interesting graphs would be obtained than those presented in the chapter IV. Also system benchmarks from Åström and Hägglund can be used to test the proposed approach [22]. Other interesting system models usable for the validation of the GUI are given in [23].

A user defined time domain criteria will be also tested on real systems. The application of other considered time domain criteria is also offered here.

Another improvement is an extension for PID controllers. Clearly, a robust region will no longer come out in 2D plane but in 3D space. Its coordinates would be defined using the parameters K_p, K_i and K_d. This would increase the complexity of the whole task and make the graphs less readable. Therefore, the evaluation of the region obtained in this way using additional criteria or norms would be relatively more complicated. However, if all the calculations are performed inside the application and the user only controls it by using the GUI, then it is not an obstacle for him. Next, the ratio between integral and derivative term can be fixed and move back to 2D plane.

VI. Conclusion

In this paper, the PI controller design procedure was introduced utilizing a combination of frequency-domain methods with time-domain criteria. Specifically, Nyquist plot shaping conditions are considered. The result is a robust region containing all controller parameters fulfilling given set of requirements. The obtained region was numerically processed in Matlab and Simulink and each controller was numerically evaluated by a given time-domain criterion or system norms. The resulting 3D graphs subsequently provide a visualization that can be easily used and interpreted. A GUI program was

created in Matlab. It contains all the calculation procedures, and the user does not have to deal with them again. The authors believe that such approaches will help to increase the percentage of well-tuned controllers, thus may lead to huge energy savings.

ACKNOWLEDGMENT

Authors would like to thank CHARM project "Challenging environments tolerant Smart systems for IoT. This project has received funding from the ECSEL Joint Undertaking (JU) under grant agreement No 876362 and also by H2020 ECSEL JU grant agreement No. 101007311 IMOCO4.E project *Intelligent Motion Control under Industry4.E.'* The JU receives support from the European Union's Horizon 2020 research and innovation programme and Finland, Austria, Belgium, Czechia, Germany, Italy, Latvia, Netherlands, Poland, Switzerland.

REFERENCES

[1] Karl Johan Astrom and Richard M. Murray. *Feedback Systems: An Introduction for Scientists and Engineers*. USA: Princeton University Press, 2008. ISBN: 0691135762.

[2] W. Krajewski, A. Lepschy, and U. Viaro. "Designing PI controllers for robust stability and performance". In: *IEEE Transactions on Control Systems Technology* 12.6 (2004). DOI: 10.1109/TCST.2004.833619.

[3] Martin Čech, Arend-Jan Beltman, and Kaspars Ozols. "Pushing Mechatronic Applications to the Limits via Smart Motion Control". In: *Applied Sciences* 11.18 (2021).

[4] Kiam Heong Ang, G. Chong, and Yun Li. "PID control system analysis, design, and technology". In: *IEEE Transactions on Control Systems Technology* 13.4 (2005). DOI: 10.1109/TCST.2005.847331.

[5] Yun Li, Kiam Heong Ang, and G.C.Y. Chong. "PID control system analysis and design". In: *IEEE Control Systems Magazine* 26.1 (2006). DOI: 10.1109/MCS.2006.1580152.

[6] K.S. Tang et al. "An optimal fuzzy PID controller". In: *IEEE Transactions on Industrial Electronics* 48.4 (2001). DOI: 10.1109/41.937407.

[7] Fengping Pan et al. "ITAE-optimal PI controller based on Genetic Algorithm for low-order process with large time delays". In: *2014 20th International Conference on Automation and Computing*. 2014. DOI: 10.1109/IConAC.2014.6935475.

[8] Miloš Schlegel and Pavla Medvecová. "Design of PI Controllers: H Region Approach". In: *IFAC-PapersOnLine* 51.6 (2018). 15th IFAC Conference on Programmable Devices and Embedded Systems PDeS 2018. ISSN: 2405-8963.

[9] J. Ackermann and D. Kaesbauer. "Design of robust PID controllers". In: *2001 European Control Conference (ECC)*. 2001.

[10] R.N. Tantaris, L.H. Keel, and S.P. Bhattacharyya. "H/sub /spl infin// design with first-order controllers". In: *IEEE Transactions on Automatic Control* 51.8 (2006).

[11] Martin Čech. "Robust controller design for fractional-order systems". PhD thesis. Pilsen: University of West Bohemia, 2008.

[12] Olof Garpinger, Tore Hägglund, and Karl Johan Åström. "Performance and robustness trade-offs in PID control". In: *Journal of Process Control* 24.5 (2014). ISSN: 0959-1524. DOI: https://doi.org/10.1016/j.jprocont.2014.02.020. URL: https://www.sciencedirect.com/science/article/pii/S0959152414000730.

[13] Radek Matušů, Bilal Şenol, and Libor Pekař. "Robust PI Control of Interval Plants With Gain and Phase Margin Specifications: Application to a Continuous Stirred Tank Reactor". In: *IEEE Access* 8 (2020). DOI: 10.1109/ACCESS.2020.3014684.

[14] Yuliia Kozhushko et al. "Robust Control of Battery-Supercapacitor Energy Storage System Using Kharitonov Theorem". In: *2020 IEEE 14th International Conference on Compatibility, Power Electronics and Power Engineering (CPE-POWERENG)*. Vol. 1. 2020. DOI: 10.1109/CPE-POWERENG48600.2020.9161569.

[15] Omer Turksoy et al. "Computation of Robust PI-Based Pitch Controller Parameters for Large Wind Turbines". In: *Canadian Journal of Electrical and Computer Engineering* 43.1 (2020), pp. 57–63. DOI: 10.1109/CJECE.2019.2923050.

[16] Čech. M and M Schlegel. "Generalized robust stability regions for fractional PID controllers". In: *2013 IEEE International Conference on Industrial Technology (ICIT)*. 2013, pp. 76–81.

[17] M. Čech and M. Schlegel. "Interval PID tuning rules for a fractional-order model set". In: *IFAC Proceedings Volumes*. Vol. 18. 2011. Chap. PART 1, pp. 5359–5364.

[18] M. Schlegel, M. Čech, and J. Mertl. "Generalized robustness regions for PID controllers". In: *Process Control 2003 Summaries Volume*. Štrbské Pleso, Slovak Republic, 2003.

[19] D.N. Bazylev at all. "Approaches for stabilizing of biped robots in a standing position on movable support". In: *Scientific and Technical Journal of Information Technologies, Mechanics and Optics* 15.3 (2015).

[20] Vilém Žán. "Interactive tools for computing multi-dimensional robust stability regions for simple controllers". Pilsen: University of West Bohemia, 2021.

[21] Unbehauen H. "Controller Design In Time-Domain". In: 2011.

[22] K.J. Åström and Tore Hägglund. "Revisiting the Ziegler-Nichols Step Response Method for PID Control". In: *Journal of Process Control* 14 (Sept. 2004). DOI: 10.1016/j.jprocont.2004.01.002.

[23] Donghai Li et al. "Performance Robustness Criterion of PID Controllers". In: Mar. 2012. ISBN: 978-953-51-0405-6. DOI: 10.5772/34384.